High-performance traveling-wave electroabsorption modulators utilizing mushroom-type waveguide and periodic transmission line loading

Kambiz Abedi*

Department of Electrical Engineering, Faculty of Electrical and Computer Engineering, Shahid Beheshti University, Tehran 1983963113, Iran

(Received 29 November 2011)

For the first time, periodic loaded electrodes and mushroom-type waveguide are combined to improve the performance of traveling-wave electroabsorption modulators (TWEAMs) based on the asymmetric intra-step-barrier coupled double strained quantum well (AICD-SQW). The electrical modulation response of periodic mushroom-type TWEAM is obtained by using equivalent circuit model, and is compared with simulation result of conventional mushroom-type TWEAM counterpart. The equivalent circuit model simulation results indicate that for the exemplary modulation length of 300 μm, the mushroom-type TWEAM with periodic transmission line loading can achieve much wider bandwidth about 99.7 GHz and 43.1 GHz than the conventional counterpart with about 43 GHz and 33 GHz for 35 Ω and 45 Ω terminations, respectively.

Document code: A **Article ID:** 1673-1905(2012)03-0176-3

DOI 10.1007/s11801-012-1183-3

Traveling-wave electroabsorption modulators (TWEAMs) are the key devices for optical communication system as well as analog fiber link systems and high-data-rate optical wavelength division multiplexing systems. They have some advantages, such as compact size, low chirp, high modulation frequencies, high extinction ratio, high efficiency, and easy integration with other semiconductor devices, for example, semiconductor lasers, optical amplifiers and passive components[1-4]. The utilization of traveling-wave (TW) electrodes for EAMs can significantly enhance the bandwidths compared with the traditional lumped-element type devices. However, one drawback of TWEAMs is the low characteristic impedance of the transmission line compared with 50 Ω electrical drivers, due to the high capacitive loading of the p-n junction. The high capacitance also results in slow-wave mode propagation[5] of the electrical signal, which limits the maximum interaction length between the electrical and optical waves. Recently, one of the methods has been reported for reducing the capacitance per unit length of TW-EAMs including periodic transmission line loading[6-8].

Modulation length and capacitance in the optical waveguide are segmented and connected to the transmission line periodically as capacitive loading through the metal bridges, which lowers the microwave velocity and impedance.

In the previous paper, we have proposed an asymmetric intra-step-barrier coupled double strained quantum well (AICD-SQW) structure which has some advantages, such as very low insertion loss, zero chirp, large Stark shift, high extinction ratio, and higher figures of merit in comparison with the intra-step quantum well (IQW) structure[9,10]. Recently, we investigated the modulation response of mushroom-type TWEAM with AICD-SQW active region using equivalent circuit model by considering the interaction between microwave and optical fields in waveguide, and compared with conventional ridge-type TWEAM[11]. In this paper, we utilize both the periodic transmission line loading and mushroom-type waveguide to develop high-performance TW-EAMs based on AICD-SQW active layer. Using equivalent circuit model, the modulation response of mushroom-type TWEAM with periodic transmission line is analyzed and compared with conventional mushroom-type TWEAM.

The frequency response of a periodic traveling-wave modulator is limited not only by the mismatch of impedance and velocity, but also by the microwave loss, the microwave dispersion and filtering effects due to the periodic capacitive loading and various parasitic effects. To analyze the modulation response, we can use a microwave equivalent circuit model for the periodic traveling-wave electrode, as shown in Fig.1[11].

* E-mail: k_abedi@sbu.ac.ir

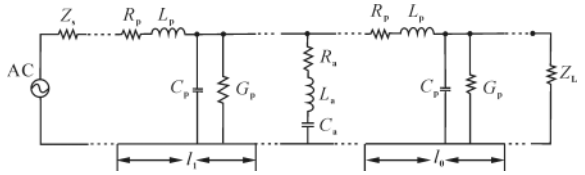

Fig.1 Equivalent circuit model of TWEAM with periodic transmission line

It represents an active modulation waveguide with N segments periodically shunting with a transmission line. Since each active segment is usually very short, it can be modeled by a lumped $L_aR_aC_a$ circuit. The inductance L_a is induced by the connection bridge, the resistance R_a includes the metal bridge resistance and the series resistance of the modulation waveguide, and the capacitance C_a is the junction capacitance of the modulation waveguide. It is the voltage across the capacitance C_a that does the actual modulation.

The microwave transmission line length between any two adjacent bridges is l_0=50 μm. The microwave source impedance Z_s and the termination impedance are both typically 50 Ω. The *RLGC* equivalent circuit model is utilized for passive transmission line. The per-unit-length *RLGC* parameters shown in Fig.2 can be expressed as

$$R_{\mathrm{P}} = \mathrm{Re}(Z_{0\mathrm{p}}\gamma_{\mu\mathrm{p}}l_{\mathrm{p}}), \quad L_{\mathrm{P}} = \frac{\mathrm{Im}(Z_{0\mathrm{p}}\gamma_{\mu\mathrm{p}}l_{\mathrm{p}})}{\omega},$$

$$G_{\mathrm{P}} = \mathrm{Re}(\frac{\gamma_{\mu\mathrm{p}}l_{\mathrm{p}}}{Z_{0\mathrm{p}}}), \quad C_{\mathrm{P}} = \frac{\mathrm{Im}(\frac{\gamma_{\mu\mathrm{p}}l_{\mathrm{p}}}{Z_{0\mathrm{p}}})}{\omega}, \tag{1}$$

where $Z_{0\mathrm{p}}$ and $\gamma_{\mu\mathrm{p}}$ are the characteristic impedance and the propagation constant of passive segments, respectively.

Under small-signal modulation, the modulation index for each active segment is linearly proportional to the modulation voltage across its capacitor C_a. The frequency response of the periodic loaded mushroom-type TWEAM is therefore proportional to the square of the summation of modulation voltages across all the capacitors multiplied by a phase factor caused by the traveling of the modulated optical wave envelope. The normalized frequency response of the periodical loaded mushroom-type TWEAM is[7,8]:

$$M(f) = \left| \frac{2}{NVs} \sum_{n=1}^{N} VC_n \, \mathrm{e}^{\mathrm{j}\omega[l_1+(n-1)l_0]/v_0} \right|^2, \tag{2}$$

where VC_n is the modulation voltage across the nth capacitor, $\exp\{\mathrm{j}\omega[l_1+(n\text{-}1)l_0]/v_0\}$ is the microwave phase factor at the nth segment due to the traveling time of the modulated optical wave envelope, v_0 is the optical group velocity in the optical waveguide, and $\frac{2}{NVs}$ is the normalization constant for the summation of the voltage. The circuit elements for active and passive segments can easily be extracted from the TWEAM transmission line microwave parameters Z_0 (characteristic impedance) and γ (propagation constant), which are obtained by full-wave simulations of the given geometry using high frequency structure simulator (HFSS) based on finite element method (FEM).

The main material elements in order to perform waveguide simulations are the refractive indices. The waveguide simulation considers 2-dimensional structures. The active region is composed of an intrinsic eight-period AICD-SQW, separated with 10 nm-thick $In_{0.52}Al_{0.48}As$ barriers[9]. The thickness of the active layer is considered to be 0.2064 μm. In order to improve the junction capacitance, we use a thin intrinsic buffer layer on top of the active layer with the thickness of 200 nm. The width of the active layer is taken as 2 μm, and the simulation is carried out with a wavelength of 1.55 μm.

The corresponding geometry values and typical material data are all in Ref.[5]. For our case study, we use the data for the InP/InGaAsP material system according to published devices[11]. The effective optical index $n_{\mathrm{o\_eff}}$ defines the optical speed, which should be known in the analysis of a traveling-wave modulator. The calculated effective optical index is 3.53. In exemplary periodic TWEAM based on AICD-SQW, the total active modulation length is assumed to be 300 μm, which is divided into 6 segments. For each active segment with the length of 50 μm, we consider C_a~29.75 f F, R_a~4.12 + 0.04 $f^{1/2}$ Ω (f in GHz) and L_a~16 pH. Fig.2 shows the real part of the characteristic impedance for passive segment. As shown in Fig.2, the characteristic impedance approaches a constant level for frequencies above 5 GHz. The passive segments transmission line with low-k dielectric material typically has a characteristic impedance of $Z_{0\mathrm{p}}$~68 Ω.

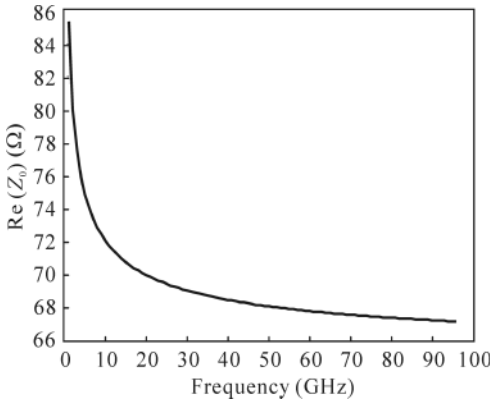

Fig.2 Real part of characteristic impedance vs. frequency

The calculated microwave velocity index for passive segment is shown in Fig.3. The microwave velocity index of passive segment (n_μ~1.4) is much smaller than the effective opti-

cal index of n_{o_eff}~3.53. Fig.4 shows the calculated microwave loss for passive segment of periodic TWEAM based on AICD-SQW using HFSS through FEM. As shown in Fig.4, the microwave loss increases strongly with frequency.

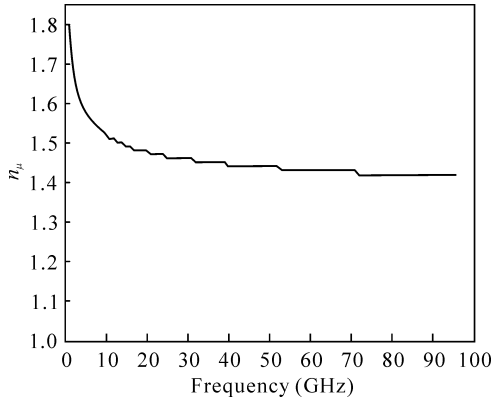

Fig.3 Microwave index vs. frequency

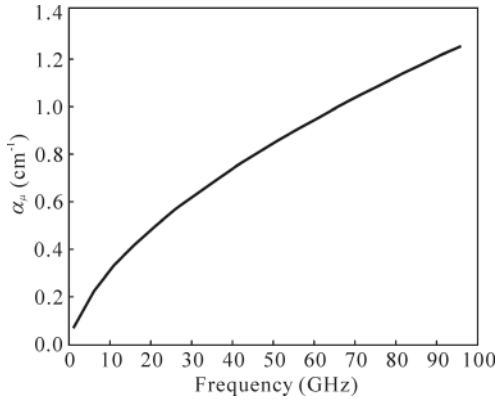

Fig.4 Microwave loss vs. frequency

We first calculate the frequency response of the periodic mushroom-type TWEAM based on AICD-SQW active layer with 35 Ω and 45 Ω terminations. The resulted 3 dB bandwidths are 99.7 GHz and 43.1 GHz, respectively, as shown in Fig.5. Using the same waveguide design and the total modulation length of 300 μm, we also calculate the frequency response for the conventional mushroom-type TWEAM, and the results are plotted in Fig.5. Only the bandwidths of 43 GHz and 33 GHz can be achieved when the conventional mushroom-type TWEAM is terminated by the resistors with 35 Ω and 45 Ω, respectively. The penalty for the periodic TWEAM

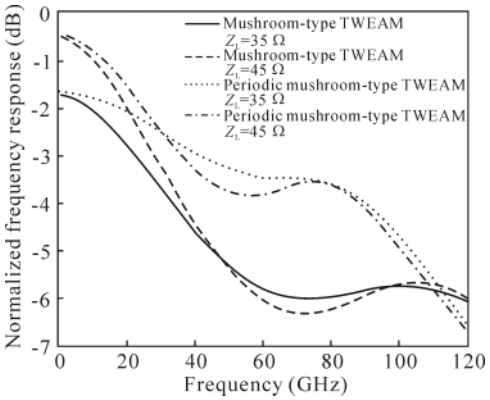

Fig.5 Calculated frequency responses for the periodic and conventional mushroom-type TWEAMs with the total active modulation length of 300 μm and the terminations of 35 Ω and 45 Ω

is some extra optical loss due to the passive optical waveguide. Fortunately, the optical loss can be significantly decreased using the AICD-SQW structure as the active layer of periodic TWEAM.

References

[1] L. P. Hou Li, W. Wang and H. L. Zhu, Optoelectron. Lett. **1**, 83 (2005).

[2] Y.-J. Chiu, H.-F. Chou, V. Kaman, P. Abraham and J. E. Bowers, IEEE Photon. Technol. Lett. **14**, 792 (2002).

[3] S. Irmscher, R. Lewen and U. Eriksson, IEEE Photon. Technol. Lett. **14**, 923 (2002).

[4] J. Lim, Y.-S. Kang, K.-S. Choi, J.-H. Lee, S.-B. Kim and J. Kim, IEEE J. Lightw. Technol. **21**, 3004 (2003).

[5] R. Lewén, S. Irmscher and U. Eriksson, IEEE Trans. Microwave Theory Technol. **51**, 1117 (2003).

[6] R. Lewén, S. Irmscher, U. Westergren, L. Thylén and U. Erikssons, IEEE J. Lightw. Technol. **22**, 172 (2004).

[7] G. L. Li, T. G. B. Mason and P. K. L. Yu, IEEE J. Lightw. Technol. **22**, 1789 (2004).

[8] Y. Tang, Y. Yu, Y. Ye, U. Westergren and S. He., Opt. Commun. **281**, 5177 (2008).

[9] K. Abedi, V. Ahmadi, E. Darabi, M. K. Moravvej-Farshi and M. H. Sheikhi, Solid State Electron. **53**, 312 (2008).

[10] K. Abedi, Eur. Phys. J. Appl. Phys. **56**, 10403 (2011).

[11] K. Abedi, V. Ahmadi and M. K. Moravvej-Farshi, Opt. Quant. Electron. **41,** 719 (2009).